

Length of adaptive walk on uncorrelated and correlated fitness landscapes

Sarada Seetharaman and Kavita Jain

Theoretical Sciences Unit, Jawaharlal Nehru Centre for Advanced Scientific Research, Jakkur P.O., Bangalore 560064, India

(Dated: July 11, 2021)

We consider the adaptation dynamics of an asexual population that walks uphill on a rugged fitness landscape which is endowed with large number of local fitness peaks. We work in a parameter regime where only those mutants that are single mutation away are accessible, as a result of which the population eventually gets trapped at a local fitness maximum and the adaptive walk terminates. We study how the number of adaptive steps taken by the population before reaching a local fitness peak depends on the initial fitness of the population, the extreme value distribution of the beneficial mutations and correlations amongst the fitnesses. Assuming that the relative fitness difference between successive steps is small, we analytically calculate the average walk length for both uncorrelated and correlated fitnesses in all extreme value domains for a given initial fitness. We present numerical results for the model where the fitness differences can be large, and find that the walk length behavior differs from that in the former model in the Fréchet domain of extreme value theory. We also discuss the relevance of our results to microbial experiments.

PACS numbers: 87.23.Kg, 02.50.Cw, 02.50.Ey

I. INTRODUCTION

Fitness is a quantitative measure of how successful an organism is in a given environment - an organism with high fitness has a better chance of propagation within the population than those with lower fitness. Fitness landscape defined as a map from genetic sequences to (genotypic) fitness is a fundamental concept in the theory of biological evolution [1, 2]. But to construct a fitness landscape for a microbe with merely hundred nucleotide sequence, one needs to experimentally measure the fitness of $4^{100} \sim 10^{60}$ sequences which is not possible with the current technology. However some empirical insights have been obtained regarding the qualitative nature of the fitness landscapes in the recent years. Fitness have been measured for various microbes for a small part (up to ten loci) of the genome which gives information about the local topography of the fitness landscape [3]. Large scale fitness landscapes for about 70,000 HIV sequences have also been constructed [4]. A key result which has emerged from these empirical studies is that the fitness landscapes are quite rugged *i.e.* they are endowed with moderately large number of local fitness peaks which are sequences fitter than their nearest neighbours. A related characteristic of such fitness landscapes is that they are partially correlated [5, 6] which has the effect of reducing the number of local fitness peaks relative to a fully uncorrelated fitness landscape.

Besides measuring fitness landscapes directly, the dynamics of adaptation have also been exploited to obtain insights into the structure of the underlying fitness landscape [6–10]. During adaptation, a population climbs the fitness landscape, and in asexual populations, this process occurs exclusively via beneficial mutations. However as advantageous mutations are rare, accounting for less than 15% of all mutations [11, 12], experimental study of adaptation is difficult. But in recent times, it has been possible to track adaptive trajectories for several tens to thousands of generations, especially in microbial populations [10]. It has been observed that initially the population evolves quickly and then its fitness increases slowly towards different fitness plateau for the same initial fitness [8, 13, 14] thus supporting the conclusion that fitness landscapes are rugged. On such fitness landscapes, while very large populations can reach the global fitness maximum quickly as they produce greater number of mutants, smaller populations stay trapped at a local fitness peak for a long time [9, 15–17]. In recent experiments, the number of adaptive mutations that occur till the population reaches a fitness plateau have been measured, and it has been found that the population encounters a local fitness maximum within two [18] to nine [19] substitutions.

In this article, we address how the number of adaptive steps that a population takes before it gets trapped at a local fitness peak depends on the properties of the underlying fitness landscape. We consider an asexual population in the *strong selection-weak mutation* regime where the rate of mutations is low enough to produce only those sequences that are single mutation away (weak mutation), and a mutation that confers a fitness benefit has a substantial probability of spreading through the population while the neutral or disadvantageous mutations get lost (strong selection). As a result of these assumptions, the entire population can be represented by a single point in the fitness landscape, and performs an uphill *adaptive walk* which terminates once the population reaches a local fitness peak since a better fitness is at least two mutations away [20, 21]. The properties of the adaptive walk depend on the distribution of beneficial mutations which can be found by appealing to the extreme value theory (EVT) [21] since beneficial mutations are rare and therefore lie in the tail of the full fitness distribution [11, 12]. For independent and identically distributed (i.i.d.) random variables, the EVT states that the distribution of the tails can belong to one of the three domains

namely Weibull, Gumbel and Fréchet [22]. Interestingly, all the three extreme value domains have been observed in recent experiments. Although the exponential distribution for beneficial mutations belonging to the Gumbel domain has been most commonly seen [24–27], the fitness distribution of beneficial mutations belonging to Weibull [19, 28] and Fréchet [29] domains have also been observed. Here we study how the walk length depends on these three extreme value domains. Although, as mentioned above, fitnesses are known to be correlated, much of the previous work on the subject ignores correlations completely [24, 31–33]. Here we also investigate how correlations affect the number of adaptive substitutions. Motivated by recent experiments on adaptive walks in which a maladapted population starts at different fitness [18, 19, 34], we also analyse the dependence of the walk length on the initial fitness.

According to the population genetics theory [35], the probability that a beneficial mutation will spread through the population increases with the relative fitness difference between the mutant and the parent exponentially fast towards unity. Using this probability function, we numerically find that the adaptive walk is shortest in the Gumbel domain [30]. However when the relative fitness difference is assumed to be small, this probability is proportional to the relative fitness difference, and in this case, we find that the adaptive walks are shortest in the Fréchet domain and longest in the Weibull domain. Although the assumption of small fitness differences is biologically incorrect, especially in the Fréchet domain, it is still interesting to consider this model as it connects to other systems [32], such as deterministically evolving populations [36, 37] and a gas of particles undergoing elastic collisions [38, 39], and lends itself to analytical calculations. We calculate the average walk length in all the three EVT domains for uncorrelated fitnesses, and show that it depends logarithmically on the initial rank of the population. Using results from the large deviation theory [40], we also obtain analytical expressions for the walk length for correlated fitnesses, and find that the walk lasts longer on correlated fitness landscapes as they have fewer local fitness peaks.

The article is organised as follows: In Sec. II, we describe the model of fitness landscapes and adaptation dynamics employed here. We present a detailed analysis of the model which assumes the fitness difference to be small on uncorrelated and correlated fitness landscapes in Sec. III, and then move on to describe our numerical results for the full model that takes care of large relative fitness differences in Sec. IV. We finally conclude with a summary of our results, and their relevance to the experiments.

II. MODEL

A. Fitness landscapes

The adaptation model studied here is defined on a hypercube of dimension L where each vertex corresponds to a binary sequence, as shown in Fig. 1 for $L = 4$. Each sequence is assigned a fitness which is an i.i.d. random variable chosen from a probability distribution. Experiments indicate that deleterious and neutral mutations account for most of the weight in the fitness distribution, but a significant fraction comes from the beneficial mutations as well [11]. Since the adaptation process is governed by these rare beneficial mutations, we need to consider the upper tail of the fitness distribution [21] which immediately suggests the use of the extreme value theory and the related peak-over-thresholds formulation described below [22, 31].

Consider the conditional cumulative distribution $P_{f_T}(f)$ for the fitness f chosen from the distribution $\hat{p}(f)$ above a large threshold f_T which here refers to the wild type fitness. Formally, we have

$$P_{f_T}(f) = \text{Prob}(F - f_T < f | F > f_T) \quad (1)$$

$$= 1 - \frac{\hat{q}(f + f_T)}{\hat{q}(f_T)} \quad (2)$$

where $\hat{q}(f) = \int_f dg \hat{p}(g)$. For large enough thresholds, the above cumulative distribution approaches the Generalised Pareto Distribution (GPD) [22]:

$$P_{f_T}(f) \xrightarrow{\text{large } f_T} P(f, \tau) = 1 - \left[1 + \frac{\kappa f}{\tau} \right]^{-1/\kappa}, \quad -\infty < \kappa < \infty \quad (3)$$

where τ is a scale factor and the shape parameter κ can take any real value. The limiting distribution with positive κ corresponds to a power law distribution, and is obtained when $\hat{p}(f)$ itself decays algebraically. When $\kappa < 0$, the fitness distribution (3) makes sense when $f < -\tau/\kappa$ and therefore such a distribution is bounded above. This class of distributions appears when $\hat{p}(f)$ is truncated. Finally, the limit $\kappa \rightarrow 0$ gives an exponentially decaying function which is obtained from unbounded distributions decaying faster than a power law. For example, for the fitness distribution

$\hat{p}(f) = cf^{c-1} e^{-f^c}$, $c > 0$, the conditional distribution works out to be

$$P_{f_T}(f) = 1 - \frac{e^{-(f+f_T)^c}}{e^{-f_T^c}} \quad (4)$$

$$\approx 1 - e^{-cf_T^{c-1}f}, \quad f_T \gg 1 \quad (5)$$

Thus the tail of the conditional distribution is an exponential, and the threshold fitness f_T and the exponent c characterising the tail of the full distribution $\hat{p}(f)$ appear in the scale factor τ . In summary, the distribution $p(f, \tau) = dP(f, \tau)/df$ of *beneficial* mutations for i.i.d. fitnesses is a GPD, or in the language of the extreme value theory, the distribution $p(f, \tau)$ can be of only three types viz., Weibull ($\kappa < 0$), Gumbel ($\kappa \rightarrow 0$) and Fréchet ($\kappa > 0$) [22]. A result from the extreme value theory that we will need for subsequent discussion is regarding the largest value of L random variables, or in other words, the typical fitness \tilde{f} of a local fitness peak. Since, in a set of L random variables, the number of fitnesses that exceed \tilde{f} is one, we have [22]

$$L \int_{\tilde{f}}^u df p(f) = 1 \quad (6)$$

where u is the upper limit of the fitness distribution. This immediately yields

$$\tilde{f} = \tau \left(\frac{L^\kappa - 1}{\kappa} \right) \quad (7)$$

We will set $\tau = 1$ in the rest of this article and denote the fitness distribution by $p(f)$. As we are interested in adaptive changes, an uncorrelated fitness landscape is generated by choosing fitnesses independently from $p(f)$.

We introduce correlations between sequence fitnesses using a block model [41], where a sequence of length L is assumed to be built of B blocks, each of length $L_B = L/B$. The 2^{L_B} fitnesses of each of the B blocks is an i.i.d. random variable chosen from GPD and the fitness of the whole sequence is given by the average of the block fitnesses. Fitness correlations arise because of common blocks between two sequences and can be changed by tuning the number of blocks in the sequence. The two limits namely $B = 1$ and $B = L$ produce fully uncorrelated and fully correlated fitness landscapes respectively. A measure of the ruggedness of a fitness landscape is the number of local fitness peaks (defined as sequences fitter than all of their one mutant neighbours) which decreases as the fitness correlations increase [41]. On correlated fitness landscapes, a local fitness peak is reached when the fitness of each block is a local fitness maximum. As the probability of one of the 2^{L_B} sequences being a local fitness peak is $2^{L_B}/(L_B + 1)$, the average number of local peaks on a correlated fitness landscape is given by $\left(\frac{2^{L_B}}{L_B + 1} \right)^B$ [41]. Thus on a fully correlated fitness landscape, there is only one local (same as global) fitness peak, whereas on fully uncorrelated fitness landscapes, there are on an average $2^L/(L + 1)$ local fitness maxima.

B. Adaptive walk

We consider an asexual population initially localised at a sequence with fitness f_0 in the strong selection-weak mutation regime [21] in which only the beneficial mutations spread through the population and the mutation rates are small enough so that only those sequences that are one mutation away from the currently occupied sequence can be accessed. As illustrated in Fig. 1 for sequence space of dimension 4, starting from the sequence {0000}, at the first step in the walk, the population has three fitter neighbors viz. {0010}, {0100} and {1000}, and it chooses one of them according to a stochastic rule described below. After the first step is taken, the population again scans its nearest neighbors and walks to a fitter neighbor. This process repeats until a local fitness peak is reached whereupon the adaptive walk terminates since the next beneficial mutation is at least two mutations away which is not accessible in the weak mutation regime. The number of steps taken from the initial sequence to a local fitness peak is termed as the *walk length*. In Fig. 1, two walks to the local fitness peak {0100} with length one and three are shown. Of course, an adaptive walk to a different local fitness peak (say, sequence {1001}) is also possible.

We now discuss the stochastic rules by which a nearest fitter sequence may be chosen [42]. Perhaps the simplest algorithm is the *greedy adaptive walk* (GAW) in which the fittest mutant is chosen at any step in the walk. The average length \bar{J} of the GAW has been calculated by appealing to the theory of records, and for infinitely long sequences, it turns out that [42]

$$\bar{J}_{GAW} = e - 1 \approx 1.718 \quad (8)$$

for any fitness distribution. In contrast, in the *random adaptive walk* (RAW), any fitter one-mutant is equally likely to be chosen and in this case, the average length of the walk diverges with the sequence length. More precisely, the average walk length for zero initial fitness is given by [44]

$$\bar{J}_{RAW} \approx \ln L + 1.099 \quad (9)$$

and is independent of the choice of the fitness distribution. Here we are interested in the biologically relevant situation where, as one would intuitively expect, a mutant which is much fitter than the wild type has a higher chance of sweeping through the population than a mutant which is mildly fitter. From the population genetics theory [35], it is known that in a large adapting asexual population, if h is the fitness of the wild type and $f > h$ is the fitness of the mutant, the probability that the mutant will take over the population is given by

$$\pi(f, h) = 1 - \exp\left[-\frac{2(f-h)}{h}\right] \quad (10)$$

Thus, as in Fig. 1, when several of the L nearest mutants are beneficial, the population moves to one of them with a probability proportional to π . The normalised transition probability is then given by [30, 45, 46]

$$T(f \leftarrow h) = \frac{1 - e^{-\frac{2(f-h)}{h}}}{\sum_{g>h} 1 - e^{-\frac{2(g-h)}{h}}} \quad (\text{full model}) \quad (11)$$

The above equation is clearly nonlinear in the fitnesses, and we have not been able to obtain analytical results using the above transition probability. However our previous work [30] shows that when $\kappa \leq 0$, the relative fitness difference $s = (f-h)/h$ between the mutations encountered is small, and we may therefore write $\pi(f, h) \approx 2s$ [20, 21, 45, 46] which gives us

$$T(f \leftarrow h) = \frac{f-h}{\sum_{g>h} g-h} \quad (\text{linear model}) \quad (12)$$

In this article, we shall refer to the model that uses (11) as the *full model* and present numerical results for it in Sec. IV. In the next section, we will study in detail the *linear model* that employs (12) for all κ . The linear model is interesting to study, not only because it is amenable to analysis, but also because the results obtained here appear in other systems [32] viz. models of deterministically evolving populations [36, 37, 47] and the Jepsen gas that describes a system of particles with random velocities undergoing elastic collisions [38, 39]. Two variants of the linear model have been studied: while [20] and [32] considered adaptation in a single fixed neighborhood where the mutants are produced only at the first step and the same are retained all through the walk, the model studied in [24, 30, 31, 33, 45] assumes that a new set of L fitnesses (corresponding to the fitness of the one mutant neighbours) are generated at each step of the walk. Though we shall use the latter model here, it is interesting to note that most results for the walk length are robust with respect to this assumption.

III. WALK LENGTH IN THE LINEAR MODEL

A. On uncorrelated fitness landscapes

For zero initial fitness, it has been shown that if the mean \bar{f} of the fitness distribution $p(f)$ is finite, the walk length increases with the length of the sequence but remains constant otherwise [33, 45]. To understand this transition at $\kappa = 1$ above which \bar{f} is infinite, here we present a simple argument and refer the reader to [33] for details. For $\kappa < 1$, as the transition probability (12) is nonzero for finite fitness differences, the adaptive walk goes on indefinitely for infinitely long sequence or in other words, the adaptive walk length diverges with the sequence length L . A calculation for zero initial fitness and large L shows that the walk length cumulants increase logarithmically with the sequence length [33]. In particular, the mean walk length \bar{J} increases as [32, 33, 45]

$$\bar{J}(L|f_0 = 0) \approx \beta_\kappa \ln L \quad (13)$$

where

$$\beta_\kappa = \frac{1-\kappa}{2-\kappa}, \quad \kappa < 1 \quad (14)$$

which shows that the walks are shorter for slowly decaying fitness distributions. For $\kappa > 1$, as the mean of the fitness distribution is infinite, the normalisation sum in the denominator on the right hand side (RHS) of (12) is dominated by the largest value \tilde{f} amongst L i.i.d. random variables (refer (7)). This implies that the transition occurs to one of the highly fit sequences with fitness of order \tilde{f} . Since the number of such sequences is of order unity, the walk terminates in a few steps resulting in a constant walk length.

As shown in Fig. 2, a similar transition is seen at $\kappa = 1$ when the sequence length is kept fixed and the initial fitness is varied. We now generalise the calculation in [33] for zero initial fitness to find how the average walk length changes with the initial fitness when $\kappa < 1$. Since the mean of the fitness distribution is finite when κ is below unity, for long sequences, we can write (12) as [45]

$$T(f \leftarrow h) = \frac{p(f) (f - h)}{\int_h^u dg p(g) (g - h)} \quad (15)$$

using which we will calculate the walk length as detailed below.

An adaptive walk will stop at step J if all the L neighbouring sequences have a fitness lower than that of the currently occupied sequence. Thus if $Q_J(L|f_0)$ is the probability that the adaptive walk of a sequence of length L lasts exactly J steps, we can write [45]

$$Q_J(L|f_0) = \int_{f_0}^u df q^L(f) \mathcal{P}_J(f|f_0) \quad (16)$$

where $\mathcal{P}_J(f|f_0)$ is the probability distribution of the fitness f at the J th step, given the initial fitness f_0 which satisfies (A1), and $q(f)$ is the cumulative probability of having a fitness lower than f which is given by

$$q(f) = \int_0^f dg p(g) = 1 - (1 + \kappa f)^{-1/\kappa} \quad (17)$$

For the transition probability (15), the integral equation (A1) for the distribution $\mathcal{P}_J(f|f_0)$ appearing in (16) can be recast as a second order differential equation for the distribution $P_J(f|f_0)$ defined through $\mathcal{P}_J(f|f_0) = p(f)P_J(f|f_0)$, and is given by [45]

$$P''_{J+1}(f|f_0) = \frac{p(f)(1 - q^L(f))}{\int_f^u dg (g - f) p(g)} P_J(f|f_0), \quad J \geq 1 \quad (18)$$

where the prime refers to a derivative with respect to (w.r.t.) f . Although we are unable to analyse (18) when L is finite, as explained below, it is possible to extract useful information from it when the sequence is infinitely long and using the fact that for a finite sequence, there is a characteristic fitness scale \tilde{f} given by (7).

We first introduce the generating function $G(x, f) = \sum_{J=1}^{\infty} P_J(f) x^J$, $x < 1$ which, due to (18), obeys the following differential equation:

$$G''(x, f) = \frac{x(1 - \kappa)(1 - q^L(f))}{(1 + \kappa f)^2} G(x, f) \quad (19)$$

and is subject to the initial conditions (A5) and (A6). In the above equation, the cumulative probability $q^L(f)$ of the maximum value distribution is a smoothly varying function that increases from zero to one, as the fitness f increases and belongs to one of the three EVT domains. For the cumulative fitness distribution (3), we find that for large L [22]

$$q^L(f) \approx e^{-\left(\frac{1+\kappa f}{1+\kappa \tilde{f}}\right)^{-\frac{1}{\kappa}}} = \begin{cases} e^{-z^{-\frac{1}{\kappa}}}, & \kappa < 0 \quad (\text{Weibull}) \\ e^{-e^{-z}}, & \kappa \rightarrow 0 \quad (\text{Gumbel}) \\ e^{-z^{-\frac{1}{\kappa}}}, & \kappa > 0 \quad (\text{Fréchet}) \end{cases} \quad (20a)$$

$$(20b)$$

$$(20c)$$

where

$$z(f) = \begin{cases} f - \tilde{f} & , \kappa \rightarrow 0 \\ (1 + \kappa f)(1 + \kappa \tilde{f})^{-1} & , \kappa \neq 0 \end{cases} \quad (21a)$$

$$(21b)$$

It is useful to consider (19) as a function of z defined above. If $\tilde{z} \equiv z(\tilde{f})$, the general solution of the differential equation (19) may be written as

$$G(x, z) = \begin{cases} a_1 g_1(x, z) + a_2 g_2(x, z) & , z < \tilde{z} \\ b_1 h_1(x, z) + b_2 h_2(x, z) & , z > \tilde{z} \end{cases} \quad (22a)$$

where g_i, h_i satisfy (19), and the constants a_1, a_2 are determined in Appendix A using the initial conditions at $z_0 \equiv z(f_0) < \tilde{z}$. The other constants of integration b_1, b_2 can be found by matching the solution $G(x, z)$ and its first derivative (w.r.t. z) at $z = \tilde{z}$. Noting that \tilde{z} is constant in L and f_0 but z_0 depends on them, we find that the constants b_1, b_2 are of the form

$$b_i = b_{i1}(x)a_1(z_0) + b_{i2}(x)a_2(z_0) , \quad i = 1, 2 \quad (23)$$

To find the properties of the walk length, we next define a generating function H for the walk length distribution (16) as

$$H(x, L) = \sum_{J=1}^{\infty} Q_J(L|f_0) x^J \quad (24)$$

$$= \int_{z(f_0)}^{z(u)} dz p(z) \frac{dz}{df} q^L(z) G(x, z) \quad (25)$$

On approximating $q^L(z)$ for $z < \tilde{z}$ by zero, we get

$$H(x, L) \approx \int_{\tilde{z}}^{z(u)} dz p(z) \frac{dz}{df} q_{>}^L(z) G_{>}(x, z) \quad (26)$$

where the subscript $>$ is used to denote the quantities when $z > \tilde{z}$. Using (21) and (23), we can extract the z_0 -dependence of the generating function and find that

$$H(x, L) = \begin{cases} a_1(z_0)R_1(x) + a_2(z_0)R_2(x) & , \kappa \rightarrow 0 \\ \frac{\kappa}{1 + \kappa \tilde{f}} (a_1(z_0)R_1(x) + a_2(z_0)R_2(x)) & , \kappa \neq 0 \end{cases} \quad (27a)$$

where

$$R_i(x) = \int_{\tilde{z}}^{z(u)} dz p(z) q_{>}^L(z) \sum_{j=1}^2 b_{ji} h_j(x, z) \quad (28)$$

is independent of L and f_0 . Furthermore, from the explicit expressions for a_1 and a_2 given in Appendix A, we see that a_2 decays more rapidly with L than a_1 , and therefore we may neglect the second term on the RHS of (27a) and (27b) for large L . Since the n th cumulant μ_n of the walk length is given by [22]

$$\mu_n(L) = \left. \frac{d^n \ln H}{dX^n} \right|_{X=0} \quad (29)$$

where $X = \ln x$, to leading order in L , we finally obtain

$$\mu_n(L) \approx \begin{cases} (\ln L - f_0) \frac{d^n}{dX^n} e^{X/2} \Big|_{X=0} & , \kappa \rightarrow 0 \\ \frac{1}{2\kappa} \ln \left(\frac{L^\kappa}{1 + \kappa f_0} \right) \frac{d^n}{dX^n} \sqrt{\kappa^2 + 4e^X(1 - \kappa)} \Big|_{X=0} & , \kappa \neq 0 \end{cases} \quad (30a)$$

$$\quad (30b)$$

Setting $n = 1$ in our final result (30), we find the average walk length to be

$$\bar{J}(L|f_0) = \beta_\kappa \left(\ln L - \frac{1}{\kappa} \ln(1 + \kappa f_0) \right) + c_\kappa \quad (31)$$

where β_κ is given by (14) and the constant c_κ in which the subleading corrections in L are subsumed is determined numerically. We check that the results of [45] and [33] for $f_0 = 0$ are reproduced from the above equation. We also note that since the *typical* rank m of a fitness (with the fittest ranked one) is given by [22]

$$m = \frac{L}{(1 + \kappa f_0)^{\frac{1}{\kappa}}} = \left(\frac{1 + \kappa \tilde{f}}{1 + \kappa f_0} \right)^{\frac{1}{\kappa}} \quad (32)$$

our result (31) gives $\bar{J} = \beta_\kappa \ln m + c_\kappa$. Thus the effect of nonzero initial fitness is to replace the sequence length L in (13) for zero initial fitness (where all the mutants are fitter) by the average number of mutants present at the beginning of the walk. The logarithmic dependence of the walk length on the initial rank has been obtained in [20, 32] using a model in which both the initial rank m and the mutational neighborhood are *fixed*. Here instead the initial fitness is fixed, but the initial rank is a random variable and a new suite of mutants is generated at every step in the walk. The fact that the same basic result is obtained in the deterministic and stochastic model shows that the stochastic effects are rather unimportant on an average as noted in previous works as well [24, 32].

Our numerical results for the average walk length on uncorrelated fitness landscapes are compared with (31) in Fig. 2 where the numerical fits for constants c_κ for $\kappa = -1, 0$ and $2/3$ are 1.15, 1.21 and 1.55 respectively. We see a good match between the simulation data and (31) except when the initial fitnesses are close to the local fitness optimum where the simulation data lies below the theoretical results. This discrepancy may be due to the fact that the approximation $q(f) = 0$ is good for fitnesses far below the local fitness peak, while we have used it for all $f < \tilde{f}$ to arrive at (26).

B. On correlated fitness landscapes

In the above discussion, we have assumed that the sequence fitnesses are uncorrelated. We now discuss how the walk length changes when correlated fitnesses generated using a block model (described in the last section) are considered. If a sequence is divided into B blocks and the initial fitness of the b th block is $f_0^{(b)}$, the initial fitness of the whole sequence is given by

$$f_0 = \frac{1}{B} \sum_{b=1}^B f_0^{(b)} \quad (33)$$

Since the block fitnesses evolve independently, the average walk length is the sum of the mutations accumulated by each block [41, 45]. Thus the average walk length \bar{J}_B for a sequence composed of B blocks is given by

$$\bar{J}_B(L|f_0) = \sum_{b=1}^B \bar{J}(L_B|f_0^{(b)}) \quad (34)$$

where $\bar{J}(L_B|f_0^{(b)})$ is the average walk length for a sequence of length L_B with initial fitness $f_0^{(b)}$ on uncorrelated fitness landscapes. In the simplest situation where the initial fitness $f_0^{(b)}$ of each block is same, we immediately have [41, 45]

$$\bar{J}_B(L|f_0) = B\bar{J}(L_B|f_0) \quad (35)$$

However if the block fitnesses are random variables that satisfy (33), an average over the joint distribution $P_B(\{f_0^{(b)}\})$ of block fitnesses is also required. We thus have

$$\bar{J}_B(L|f_0) = \int_0^u df_0^{(1)} \dots \int_0^u df_0^{(B)} P_B(\{f_0^{(b)}\}) \sum_{b=1}^B \bar{J}(L_B|f_0^{(b)}) \quad (36)$$

Since the block fitnesses are i.i.d. random variables subject to the constraint (33), the distribution of block fitnesses can be written as

$$P_B(\{f_0^{(b)}\}) = \frac{\prod_{b=1}^B p(f_0^{(b)})}{\mathcal{N}_B(Bf_0)} \delta(Bf_0 - \sum_{i=1}^B f_0^{(i)}) \quad (37)$$

where the normalisation constant $\mathcal{N}_B(X)$ is the distribution of the sum of B random variables given by

$$\mathcal{N}_B(X) = \int_0^u df_0^{(1)} \dots \int_0^u df_0^{(B)} \prod_{b=1}^B p(f_0^{(b)}) \delta \left(X - \sum_{i=1}^B f_0^{(i)} \right) \quad (38)$$

$$= \int_0^X df p(f) \mathcal{N}_{B-1}(X-f) \quad (39)$$

with $\mathcal{N}_0(f) = \delta(f)$. Thus we can express the average walk length as

$$\bar{J}_B(L|f_0) = B(\beta_\kappa \ln L_B + c_\kappa) - \frac{\beta_\kappa B \int_{l_1}^{l_2} df p(f) \ln(1 + \kappa f) \mathcal{N}_{B-1}(Bf_0 - f)}{\kappa \mathcal{N}_B(Bf_0)} \quad (40)$$

where the integration limits are $l_1 = 0, l_2 = Bf_0$ in the Gumbel and Fréchet domains. In the Weibull domain, three cases arise: (i) if $Bf_0 < u$, the limits are $l_1 = 0, l_2 = Bf_0$, (ii) if $u < Bf_0 < (B-1)u$, we have $l_1 = 0, l_2 = u$ and (iii) if $(B-1)u < Bf_0 < Bu$, the limits are $l_1 = Bf_0 - (B-1)u, l_2 = u$.

1. Exactly solvable case

For exponentially distributed fitnesses, the distribution $\mathcal{N}_B(X)$ in (38) is known exactly to be [48]

$$\mathcal{N}_B(X) = e^{-X} \frac{X^{B-1}}{(B-1)!} \quad (41)$$

Taking the limit $\kappa \rightarrow 0$ in (40), we find the average walk length as

$$\bar{J}_B(L|f_0) = B(\beta_0 \ln L_B + c_0) - B\beta_0 \frac{\int_0^{Bf_0} df e^{-f} f \mathcal{N}_{B-1}(Bf_0 - f)}{\mathcal{N}_B(Bf_0)} \quad (42)$$

$$= B(\beta_0 \ln L_B + c_0) - B\beta_0 \frac{e^{-Bf_0} (Bf_0)^B}{B! \mathcal{N}_B(Bf_0)} \quad (43)$$

$$= B\bar{J}(L_B|f_0) \quad (44)$$

which is the same as that in the case where each block fitness is f_0 (refer (35)).

2. Weakly correlated fitnesses

For $\kappa \neq 0$, it appears difficult to obtain exact expressions for the walk length for correlated fitnesses. The case of two independent blocks ($B = 2$) presents the simplest model for correlated fitnesses, and we discuss this here. The distribution $\mathcal{N}_2(X)$ of two random variables is given by

$$\mathcal{N}_2(X) = \begin{cases} \int_0^X dg p(g) p(X-g), & X < u \\ \int_{X-u}^u dg p(g) p(X-g), & X > u \end{cases} \quad (45a)$$

$$(45b)$$

For $2f_0 < u$, using (45a) in the expression (40), we get

$$\frac{\bar{J}_2(L|f_0)}{B} = \beta_\kappa \ln L_B + c_\kappa - \frac{\beta_\kappa \int_0^{2f_0} df p(f) \ln(1 + \kappa f) p(2f_0 - f)}{\kappa \int_0^{2f_0} df p(f) p(2f_0 - f)} \quad (46)$$

$$= \beta_\kappa \ln L_B + c_\kappa - \frac{\beta_\kappa}{\kappa} \ln(1 + \kappa f_0) + \frac{\beta_\kappa}{2\kappa} \mathcal{I}_\kappa(w_0) \quad (47)$$

where the integral

$$\mathcal{I}_\kappa(w_0) = \frac{\int_1^{w_0} dz \ln z z^{\frac{1-\kappa}{\kappa}} (1-z^{-1})^{-1/2}}{\int_1^{w_0} dz z^{\frac{1-\kappa}{\kappa}} (1-z^{-1})^{-1/2}} \quad (48)$$

with $w_0 = (1 + \kappa f_0)^2 / (1 + 2\kappa f_0)$. Note that for large initial fitnesses $f_0 \sim u/2$, the function $w_0 \gg 1$.

Fréchet class: For positive κ and large f_0 , an approximate expression for the integral $\mathcal{I}_\kappa(w_0)$ can be obtained after an integration by parts, and we get

$$\frac{\bar{J}_2(L|f_0)}{B} \approx \bar{J}(L_B|f_0) + \frac{\beta_\kappa}{2\kappa}(\ln w_0 - \kappa) \quad (49)$$

$$\approx \beta_\kappa \ln L_B + c_\kappa - \frac{\beta_\kappa}{2\kappa}(\ln(\kappa f_0) + \ln 2 + \kappa) \quad (50)$$

Weibull class: The integral $\mathcal{I}_\kappa(w_0)$ can be calculated exactly for uniformly distributed fitnesses and is given by

$$\mathcal{I}_{-1}(w_0) = 2 + \ln w_0 - 2\sqrt{\frac{w_0}{w_0 - 1}} \sinh^{-1}(\sqrt{w_0 - 1}) \quad (51)$$

$$\approx 2(1 - \ln 2) - \frac{\ln w_0}{2w_0}, \quad w_0 \gg 1 \quad (52)$$

For arbitrary negative κ , we note that the integral $\mathcal{I}_\kappa(w_0)$ is finite when $w_0 \rightarrow \infty$ and can be written in terms of the harmonic number $H_n = n \sum_{i=1}^{\infty} (i(n+i))^{-1}$ [49]. An integration by parts then yields

$$\mathcal{I}_\kappa(w_0) \approx H_{-\frac{1}{\kappa} - \frac{1}{2}} - H_{-\frac{1}{\kappa} - 1} + \frac{\kappa \Gamma(\frac{1}{2} - \frac{1}{\kappa})}{\sqrt{\pi} \Gamma(-\frac{1}{\kappa})} \frac{\ln w_0}{w_0^{1/|\kappa|}} \quad (53)$$

which matches the result for $\kappa = -1$ as $H_{1/2} = 2 - \ln 4$. Ignoring the last term on the RHS of the above equation which decays with f_0 , we find that the average walk length can be written as

$$\frac{\bar{J}_2(L|f_0)}{B} = \bar{J}(L_B|f_0) + \frac{\beta_\kappa}{2\kappa}(H_{-\frac{1}{\kappa} - \frac{1}{2}} - H_{-\frac{1}{\kappa} - 1}), \quad f_0 \lesssim u/2 \quad (54)$$

For $f_0 > u/2$ where $\mathcal{N}_2(X)$ is given by (45b), the integrals can be done exactly and we have

$$\frac{\bar{J}_2(L|f_0)}{B} = \beta_\kappa \ln L_B + c_\kappa - \frac{\beta_\kappa \int_{-1}^1 dh (1-h^2)^{-\frac{1+\kappa}{\kappa}} (\ln(1+\kappa f_0) + \ln(1+h))}{\int_{-1}^1 dh (1-h^2)^{-\frac{1+\kappa}{\kappa}}} \quad (55)$$

$$= \beta_\kappa \ln L_B - \frac{\beta_\kappa}{\kappa} \ln(1 + \kappa f_0) + c_\kappa + \frac{\beta_\kappa}{2\kappa}(H_{-\frac{1}{\kappa} - \frac{1}{2}} - H_{-\frac{1}{\kappa} - 1}) \quad (56)$$

$$= \bar{J}(L_B|f_0) + \frac{\beta_\kappa}{2\kappa}(H_{-\frac{1}{\kappa} - \frac{1}{2}} - H_{-\frac{1}{\kappa} - 1}), \quad f_0 > u/2 \quad (57)$$

For bounded distributions, although the walk length is continuous at initial fitness equal to $u/2$, it is interesting to note that it is not differentiable. For uniformly distributed fitnesses where exact expressions for the walk length can be calculated, the average walk length obtained from (47) and (57) is found to be the same at $f_0 = 1/2$. The first derivative of the walk length (with respect to f_0) is given by

$$\frac{d\bar{J}_2}{df_0} = \begin{cases} \frac{2\beta_{-1}}{f_0^2} \left[f_0 + \frac{1}{2} \ln(1 - 2f_0) \right] & , f_0 < 1/2 \end{cases} \quad (58a)$$

$$\frac{d\bar{J}_2}{df_0} = \begin{cases} -\frac{2\beta_{-1}}{1 - f_0} & , f_0 > 1/2 \end{cases} \quad (58b)$$

From the above equation, we see that while the derivative at $f_0 = 1/2$ obtained from (58a) is undefined, the expression (58b) yields a finite constant. For general $\kappa < 0$, the derivative of the walk length calculated using (57) is seen to be finite, while it diverges when (47) is used.

3. On strongly correlated fitness landscapes

We now turn to the situation when the block number $B \gg 1$. To calculate the integral in (40), let us first consider the integrand

$$\mathcal{F}(f) = p(f) \ln(1 + \kappa f)^{1/\kappa} \mathcal{N}_{B-1}(Bf_0 - f) \quad (59)$$

The first two factors on the RHS are obviously independent of B and f_0 . However for all $\kappa < 1$ where the fitness distribution has a finite mean \bar{f} , the last factor peaks about the mean $B(f_0 - \bar{f})$ of the sum distribution which increases with both B and f_0 . Then for large enough B and f_0 , the integrand $\mathcal{F}(f)$ gets a contribution from the *lower tail* of the sum distribution instead of the region around its mean. The behavior of the tail of the sum distribution can be obtained by applying a large deviation principle if the fitness distribution possesses all finite moments as is the case for $\kappa \leq 0$. However for power law distributions with $\kappa > 0$, the $(1/\kappa)$ -th and higher moments diverge and the large deviation principle is not applicable, and in this case, we use the result that the sum distribution decays as the fitness distribution itself [22, 40]. The fact that the central limit theorem for the sum distribution does not capture the correct behavior of the integral under question is illustrated in Appendix B for exponentially distributed fitnesses.

To calculate the walk length using the large deviation theory, we first consider a normalised distribution with support on the interval $[0, u]$ defined as

$$g(t) = \kappa(\alpha - 1)(1 + \kappa t)^{-\alpha} \quad (60)$$

where $\alpha < 1, u = -1/\kappa$ for $\kappa < 0$ and $\alpha > 1, u = \infty$ when $\kappa \geq 0$. Then the distribution of the sum of B i.i.d. random variables chosen from $g(t)$ is given by

$$I_B(X; \alpha) = \int_0^u dt^{(1)} \dots \int_0^u dt^{(B)} \prod_{j=1}^B g(t^{(j)}) \delta \left(X - \sum_{i=1}^B t^{(i)} \right) \quad (61)$$

Differentiating on both sides w.r.t. α , we get

$$\frac{\partial I_B(X; \alpha)}{\partial \alpha} = \frac{B I_B(X; \alpha)}{\alpha - 1} - B \int_0^{\min(X, u)} dt g(t) \ln(1 + \kappa t) I_{B-1}(X - t; \alpha) \quad (62)$$

The upper limit in the above integral is X for unbounded distributions. But for bounded distributions, when correlations are strong (large B), the limits in case (ii) described below (40) apply. On dividing the above equation by $I_B(X; \alpha)$, it follows that the average walk length (40) can be written as

$$\bar{J}_B(L|f_0) = B(\beta_\kappa \ln L_B + c_\kappa) - \frac{\beta_\kappa B}{\kappa} \left(\frac{1}{\alpha - 1} - \frac{\partial}{\partial \alpha} \frac{\ln I_B(Bf_0; \alpha)}{B} \right) \Big|_{\alpha=1+\frac{1}{\kappa}} \quad (63)$$

Our task is now reduced to finding the sum distribution $I_B(X)$ for the various EVT domains which we describe below. *Weibull class:* According to the large deviation principle, for large B , the distribution $I_B(X)$ is of the form [40],

$$I_B(X \simeq Bx) \sim e^{Br(x)} \quad (64)$$

where the rate function $r(x)$ can be determined as described below. On using the integral representation of the Dirac delta function in (61), we get

$$I_B(X) = \frac{1}{2\pi} \int_{-\infty}^{\infty} dk e^{ikX} \left(\int_{-\infty}^{\infty} dy e^{-iky} g(y) \right)^B \quad (65)$$

$$= \frac{1}{2\pi i} \int_{-i\infty}^{i\infty} d\omega e^{B(\omega x + \ln \tilde{g}(\omega))} \quad (66)$$

where $\tilde{g}(\omega) = \int_0^\infty dt g(t) e^{-\omega t}$ is the Laplace transform of the distribution function $g(t)$. Evaluating the RHS of (66) using the saddle point method for large B [50], we get

$$\frac{\ln I_B(X)}{B} = r(x) = \omega_* x + \ln \tilde{g}(\omega_*) \quad (67)$$

where the saddle point ω_* is real and given by

$$\frac{d \ln \tilde{g}}{d\omega} \Big|_{\omega=\omega_*} = -x \quad (68)$$

The Laplace transform of the distribution $g(t)$ in (60) is given by

$$\tilde{g}(\omega) = e^\eta [(\alpha - 1)E_\alpha(\eta) + \eta^{\alpha-1}\Gamma(2 - \alpha)] \quad (69)$$

and the function $\omega_*(f_0)$ is a solution of the equation

$$\mathcal{T}(\omega_*) = \frac{(\alpha - 1)\omega^2(E_{\alpha-1}(\eta) - E_\alpha(\eta)) - \eta^\alpha \kappa^2(\eta + \alpha - 1)\Gamma(2 - \alpha)}{\omega\kappa((\alpha - 1)\omega E_\alpha(\eta) + \eta^\alpha \kappa\Gamma(2 - \alpha))} \Big|_{\omega=\omega_*} = f_0 \quad (70)$$

where $\eta = \omega/\kappa$, $E_\alpha(\eta) = \int_1^\infty dx e^{-\eta x} x^{-\alpha}$ is the exponential integral and $\Gamma(n + 1) = n!$ is the gamma function. The function $\mathcal{T}(\omega_*)$ in the above equation decreases from its maximum value $-1/\kappa$ to zero as ω_* is increased from $-\infty$ to ∞ . Using the asymptotic expansion of the exponential integral [51], we find that

$$\mathcal{T}(\omega_*) = \begin{cases} -\kappa^{-1} + (1 - \alpha)\omega_*^{-1}, & \omega_* \rightarrow -\infty \\ \omega_*^{-1}, & \omega_* \rightarrow \infty \end{cases} \quad (71a)$$

When the initial fitness is large (small), f_0 equals the left hand side (LHS) of (70) when ω_* is negative (positive). Then using (71a) and (71b) in (67), we find the rate function to be

$$r(f_0) \approx \begin{cases} 1 + \ln((\alpha - 1)\kappa f_0) + \ln(1 - \alpha\kappa f_0) & , f_0 \ll \mathcal{T}(0) \\ 1 - \alpha - (1 - \alpha) \ln\left(\frac{1 - \alpha}{1 + \kappa f_0}\right) + \ln(\Gamma(2 - \alpha)) & , f_0 \gg \mathcal{T}(0) \end{cases} \quad (72)$$

where $\mathcal{T}(0) = (1 - \kappa)^{-1}$. The above expression for the rate function is compared against the results from numerical simulations for uniformly distributed fitnesses in the inset of Fig. 3, and we see a good agreement for $f_0 < 0.3$ and > 0.7 . For small f_0 , using (63), we obtain

$$\frac{\bar{J}_B(L|f_0)}{B} = \beta_\kappa \ln L_B + c_\kappa - \frac{\beta_\kappa f_0}{1 - (1 + \kappa)f_0} \quad (74)$$

$$\approx \bar{J}(L_B|f_0) \quad (75)$$

while for large f_0 , we get

$$\frac{\bar{J}_B(L|f_0)}{B} = \beta_\kappa \ln L_B + c_\kappa - \frac{\beta_\kappa}{\kappa}(\kappa + \ln(-\kappa) + \ln(1 + \kappa f_0) + H_{-\frac{1}{\kappa}} - \gamma) \quad (76)$$

$$= \bar{J}(L_B|f_0) - \frac{\beta_\kappa}{\kappa}(\kappa + \ln(-\kappa) + H_{-\frac{1}{\kappa}} - \gamma) \quad (77)$$

where the Euler-Mascheroni constant $\gamma \approx 0.577$. The walk length expressions above can be succinctly written as

$$\bar{J}_B(L|f_0) = \bar{J}_B(L|0) - \frac{B\beta_\kappa}{\kappa} \ln(1 + \kappa f_0) \quad (78)$$

and shows that the walk for nonzero fitness is shorter, as one would intuitively expect. For $\kappa = -1$, the equations (74) and (76) are compared against the numerical results in Fig. 3, and we see that the theoretical prediction for the walk length matches the simulation results quite well in the range of initial fitness values where the rate function agrees.

Fréchet class: In this case, the sum distribution (61) for large Bf_0 is given by [22]

$$I_B(Bf_0; \alpha) \sim Bg(Bf_0) \quad (79)$$

whose tail behavior is the same as that of the fitness distribution $g(f)$. Using this in (63), we immediately find

$$\bar{J}_B(L|f_0) = B(\beta_\kappa \ln L_B + c_\kappa) - \frac{\beta_\kappa}{\kappa}(\ln(1 + B\kappa f_0) + \kappa(B - 1)) \quad (80)$$

$$\approx B(\beta_\kappa \ln L_B + c_\kappa) - \frac{\beta_\kappa}{\kappa}(\ln(\kappa f_0) + \ln B + \kappa(B - 1)) \quad (81)$$

We note that the above answer matches with (50) for the two block model discussed in the last subsection. The above equation states that the average walk length decreases logarithmically with initial fitness but, unlike in the Weibull and Gumbel domain, the coefficient of $\ln f_0$ does not scale with the number of blocks. Thus in this case

$$\bar{J}_B(L|f_0) = \bar{J}_B(L|0) - \frac{\beta_\kappa}{\kappa} \ln(1 + B\kappa f_0) \quad (82)$$

In Fig. 4, the above expression is compared with the simulation data for $\kappa = 2/3$, and we see a good quantitative agreement between the theory and the simulations.

IV. WALK LENGTH IN THE FULL MODEL

As mentioned in Sec. IIB, the transition probability (12) used to calculate the walk length is valid only when the relative fitness difference is small. However, large fitness differences during successive steps in the walk can occur when the initial fitness is small or if the fitness distribution has a fat tail [30]. In such cases, the approximation (12) breaks down, and we should consider the full transition probability (11). We have not been able to obtain analytical results for this model, and present our simulation results below.

As in the linear model, the walks are long for the full model when the initial fitness is low or when the fitness are correlated [30]. However qualitative difference between the linear and the full model is seen with regard to the walk length dependence on the extreme value domain. As explained in Sec. III A, the divergence of the denominator on the RHS of (12) is responsible for the independence of the walk length on the initial fitness when $\kappa > 1$ in the linear model. However the normalisation constant in (11) remains finite for all κ and therefore the walk length always decreases with increasing f_0 here. The inset of Fig. 2 shows that the full model is approximated very well by the linear model in the Weibull domain, and is a reasonable approximation in the Gumbel domain. This agreement is explained by the fact that the fitness difference between successive steps are indeed small in these two domains as discussed in [30]. However in the Fréchet domain, the relative fitness differences between the successive steps in the adaptive walk can be as large as hundred [30] thus rendering the linear model invalid. For a fixed initial fitness rank, the inset of Fig. 2 shows that in the full model, the walk length increases with increasing κ in the Fréchet domain. Thus the behaviour of the walk length is nonmonotonic in κ with the minimum occurring in the Gumbel domain.

Figure 5 shows the distribution of the walk length for various κ and uncorrelated fitnesses, and we observe that as $|\kappa|$ increases, this distribution approaches the corresponding result for the random adaptive walk where the walk distribution is known to be a Poisson distribution with mean $\ln L$ [44]. A related quantity is the index of dispersion of the walk length which is the ratio of the variance to the mean which is shown in the inset of Fig. 5 and displays a nonmonotonic behaviour with the minimum occurring at $\kappa = 0$ and approaching unity for $\kappa \rightarrow \pm\infty$. A similar nonmonotonic behavior is seen in the linear model but in that case, the index of dispersion approaches unity when $\kappa \rightarrow -\infty$ and one [32].

V. CONCLUSION

In this article, we studied a model of adaptation in which beneficial mutations sweep the population sequentially as it adapts by climbing up a rugged fitness landscape. The broad question addressed here is regarding the average number of adaptive mutations that occur until the population reaches a local fitness peak. This quantity has been measured in recent experiments on various systems like bacteriophage $\phi X174$ [19], fungus *A. nidulans* [18] and bacteria *E. coli* [34]. Theoretically, the number of adaptive changes have been calculated on uncorrelated fitness landscapes for zero initial fitness [33, 45] and high initial rank [20, 32, 46]. Some studies for correlated fitnesses have also been carried out [45, 52–54]. Here we have extended the previous works and studied how the length of the adaptive walk depends on the initial fitness, extreme value domains and fitness correlations.

For the linear model that assumes small relative fitness differences in all the extreme value domains, we find that the walk length decreases with increasing initial fitness logarithmically provided the mean of the fitness distribution is finite, otherwise it remains a constant. The walks are found to be shorter for fitness distributions that decay slower - in the limit $\kappa \rightarrow \infty$, the walk length approaches the greedy walk limit (8) while in the other extreme of $\kappa \rightarrow -\infty$, it tends to the random adaptive walk (9) [31]. The logarithmic variation with the same dependence on the fitness distribution as here has also been seen in other systems [32]. On correlated fitness landscapes, the previous studies have been largely numerical [52–54], while here we have presented analytical results. Interestingly, the large deviation theory finds an application in the calculation of the walk length for correlated fitnesses. We find that, as on uncorrelated fitness landscapes, the walk length decreases with increasing initial fitness and GPD exponent κ . But increasing fitness correlations also lengthen the adaptive walk since the population encounters lesser number of local fitness peaks. Our detailed analysis shows that the walk length difference $\bar{J}_B(L|f_0) - \bar{J}_B(L|0)$ scales linearly with the number of blocks (that are a measure of correlations) in the Weibull and Gumbel domains, and shows a weaker logarithmic dependence on the number of blocks in the Fréchet domain. For the sake of completeness, we also performed simulations for $\kappa > 1$ and found that the average walk length in this case shows a linear dependence on the block number (data not shown). These results for the linear model are summarised in Table I.

For the full model that is not restricted to small relative fitness differences, we find that the walk length decreases with initial fitness for all κ , unlike in the linear model. The walk length is however seen to match quantitatively well in the Weibull domain where small fitness differences arise [30]. In contrast, in the Fréchet domain, even the qualitative trends in the two models are opposite: while the walk length decreases with increasing $\kappa (< 1)$ in the linear model, it increases in the full model. Thus in the full model, the walk is shortest in the Gumbel domain. An analytical

understanding of these results is however not available.

Experiments show that a moderately sized population reaches a fitness plateau in two to four substitutions [18, 19, 34] (although one population has been seen to gain nine beneficial mutations as well [19]) thus indicating that the adaptive walks are generally short. An inverse relationship between the initial fitness and the walk length has been observed in some experiments [19, 34] in agreement with the full model. However a constant walk length independent of initial fitness has been seen in a recent experiment [18]. As described above, the full model predicts the walk length to be a nonmonotonic function of the parameter κ . The adaptive walk is expected to last longer in the experimental set ups in which Weibull [19, 28] or Fréchet [29] domain is observed than in the ones in which the distribution of beneficial mutations has an exponential tail [24–27]. However the walk length has not been measured in these experiments, while in the walk length experiments [18, 19, 34], the extreme value domain of the beneficial mutation has not been studied and therefore presently the theoretical predictions regarding the connection between the extreme value theory and the length of the adaptive walk remains experimentally untested. Although some of the available experimental results are in qualitative agreement with the theoretical predictions described above, a quantitative comparison between the experiments and the theory seems difficult. This is because in experiments measuring the walk length, the walk is assumed to terminate if the fitness remains constant over some time period but that need not imply that the adaptation is over [19]. Besides most experiments [18] cannot measure mutations whose fitness difference is below a threshold value and miss out on mutations conferring slight benefit thus underestimating the walk length. A better understanding of the theoretical results vis-à-vis the experimental ones remains a goal for the future.

Appendix A: Solution of the generating function equation (19)

The probability distribution $\mathcal{P}_J(f|f_0)$ obeys the following recursion equation [45]

$$\mathcal{P}_{J+1}(f|f_0) = \int_{f_0}^f dh T(f \leftarrow h) (1 - q^L(h)) \mathcal{P}_J(h|f_0), \quad J \geq 0 \quad (\text{A1})$$

where $T(f \leftarrow h)$ is given by (15). The above equation simply means that the population moves from fitness h to a higher fitness f at the next step with probability $T(f \leftarrow h)$ provided at least one fitter mutant is available, the probability of whose is given by $1 - q^L(h)$. For monomorphic initial condition with fixed fitness f_0 , we have the boundary conditions

$$\mathcal{P}_J(f|f_0) = \delta(f - f_0)\delta_{J,0} \quad (\text{A2})$$

$$\mathcal{P}'_J(f_0|f_0) = T'(f \leftarrow f_0) p(f_0) (1 - q^L(f_0))\delta_{J,1} \quad (\text{A3})$$

Equation (A2) is self explanatory and (A3) is obtained by applying (A2) on the first derivative of (A1) w.r.t. f [45]. For the linear model with transition probability (15), the integral equation (A1) can be recast as a second order differential equation (18).

For infinitely long sequences, the cumulative probability distribution $q^L(h) \rightarrow 0$ and the differential equation (19) for the generating function $G(x, f)$ reduces to

$$G''(x, f) = \frac{x(1 - \kappa)}{(1 + \kappa f)^2} G(x, f) \quad (\text{A4})$$

From (A2) and (A3), we have

$$G(x, f_0) = 0 \quad (\text{A5})$$

$$G'(x, f_0) = \frac{x}{\int_{f_0}^u dg (g - f_0) p(g)} \quad (\text{A6})$$

The solution of (A4) subject to above initial conditions is given by [50]

$$G(x, f) = \frac{x(1 - \kappa)(1 + \kappa f_0)^{1/\kappa}}{\sqrt{\kappa^2 + 4x(1 - \kappa)}} \left[\left(\frac{1 + \kappa f}{1 + \kappa f_0} \right)^{\alpha_+} - \left(\frac{1 + \kappa f}{1 + \kappa f_0} \right)^{\alpha_-} \right] \quad (\text{A7})$$

where

$$\alpha_{\pm} = \frac{1}{2} \left(1 \pm \sqrt{1 + \frac{4x(1 - \kappa)}{\kappa^2}} \right) \quad (\text{A8})$$

The functions a_1, a_2 appearing in (27a) and (27b) can be calculated explicitly using the above result. In terms of z defined in (21), the solution (A7) for $\kappa \neq 0$ can be written as

$$G(x, z) = \frac{x(1-\kappa)(1+\kappa f_0)^{1/\kappa}}{\sqrt{\kappa^2 + 4x(1-\kappa)}} \left[\left(z \frac{1+\kappa \tilde{f}}{1+\kappa f_0} \right)^{\alpha^+} - \left(z \frac{1+\kappa \tilde{f}}{1+\kappa f_0} \right)^{\alpha^-} \right] \quad (\text{A9})$$

Comparing the above equation with (22a), we get

$$a_1 = \frac{x(1-\kappa)(1+\kappa f_0)^{1/\kappa}}{\sqrt{\kappa^2 + 4x(1-\kappa)}} \left(\frac{1+\kappa \tilde{f}}{1+\kappa f_0} \right)^{\alpha^+} \quad (\text{A10a})$$

$$a_2 = -\frac{x(1-\kappa)(1+\kappa f_0)^{1/\kappa}}{\sqrt{\kappa^2 + 4x(1-\kappa)}} \left(\frac{1+\kappa \tilde{f}}{1+\kappa f_0} \right)^{\alpha^-} \quad (\text{A10b})$$

For exponentially distributed fitnesses, taking the limit $\kappa \rightarrow 0$ in (A7) and using (21), we find that

$$G(x, z) = \frac{\sqrt{x}e^{f_0}}{2} \left(e^{z\sqrt{x}} e^{(\tilde{f}-f_0)\sqrt{x}} - e^{-z\sqrt{x}} e^{-(\tilde{f}-f_0)\sqrt{x}} \right) \quad (\text{A11})$$

from which we obtain

$$a_1 = \frac{\sqrt{x}e^{f_0}}{2} e^{(\tilde{f}-f_0)\sqrt{x}} \quad (\text{A12a})$$

$$a_2 = -\frac{\sqrt{x}e^{f_0}}{2} e^{-(\tilde{f}-f_0)\sqrt{x}} \quad (\text{A12b})$$

Appendix B: Walk length using Gaussian approximation for exponentially distributed fitnesses

By virtue of central limit theorem [22], the distribution $\mathcal{N}_B(X)$ of the sum of B i.i.d. random variables is given by

$$\mathcal{N}_B(X) = \frac{1}{\sqrt{2\pi B\sigma^2}} \exp \left[-\frac{(X - B\bar{f})^2}{2B\sigma^2} \right] \quad (\text{B1})$$

provided the mean \bar{f} and the variance σ^2 of the parent distribution $p(f)$ exist. Since the Gaussian distribution is a good approximation to the exact distribution of the sum when $X \sim B\bar{f} \pm \sqrt{2B\sigma^2}$, we expect that it will provide a good estimate of the walk length when $f \sim B(f_0 - f) \pm \sqrt{2B\sigma^2}$ in the integrand in (42). With increasing B , as the core of the distribution $\mathcal{N}_B(X)$ moves rightwards while the factor $f e^{-f}$ in the integrand peaks around one, the overlap is significant when $f_0 \sim 1 \mp \sqrt{2\sigma^2/B}$. Thus the Gaussian approximation for the sum distribution is likely to work well in the neighborhood of initial fitness one. This can be seen more explicitly as follows: using (B1) in the integral appearing in (42), we get

$$I_{clt} = \int_0^{Bf_0} df f e^{-f} \mathcal{N}_{B-1}(Bf_0 - f) \quad (\text{B2})$$

$$= \frac{ae^{a^2} e^{-2ab}}{\sqrt{\pi}} \left[e^{-(a-b)^2} - e^{-4a^2} + \sqrt{\pi}(a-b)(\text{erf}(a-b) - \text{erf}(2a)) \right] \quad (\text{B3})$$

where $a = \sqrt{(B-1)/2}$ and $b = (Bf_0 - B + 1)/(2a)$. For large B , using the asymptotic expansion of error function, we get

$$I_{clt} \approx \frac{ae^{a^2} e^{-2ab} e^{-(a-b)^2}}{2\sqrt{\pi}(a-b)^2} \quad (\text{B4})$$

The expression (42) for the average walk length then gives

$$\bar{J}_B(L|f_0) = B(\beta_0 \ln L_B + c_0) - \beta_0 B \frac{e^{-f_0(f_0-1)}}{(2-f_0)^2} \quad (\text{B5})$$

$$\approx B(\beta_0 \ln L_B + c_0) - B\beta_0 f_0, \quad f_0 \rightarrow 1 \quad (\text{B6})$$

Thus it is only when the initial fitness is close to unity, the Gaussian approximation captures the linear relationship between \bar{J} and f_0 correctly.

EVT domain	Dependence on initial rank	Dependence on number of blocks
Weibull, $\kappa < 0$	Logarithmic	Linear
Gumbel $\kappa \rightarrow 0$	Logarithmic	Linear
Fréchet, $0 < \kappa < 1$	Logarithmic	Logarithmic
Fréchet, $\kappa > 1$	Independent	Linear

TABLE I: Table summarising the dependence of the walk length on extreme value domains, initial fitness and fitness correlations in the linear model.

-
- [1] S. Gavrillets, *Fitness Landscapes and the Origin of Species* (Princeton University Press, New Jersey, 2004).
- [2] J. A. G. M. de Visser and J. Krug, *Nat. Rev. Genet.* **15**, 480 (2014).
- [3] I. G. Szendro, M. F. Schenk, J. Franke, J. Krug, and J. A. G. M. de Visser, *J. Stat. Mech.* , P01005 (2013).
- [4] T. Hinkley *et al.*, *Nat. Genet.* **43**, 487 (2011).
- [5] C. Carneiro and D. Hartl, *Proc. Natl. Acad. Sci. USA* **107**, 1747 (2010).
- [6] C. R. Miller, P. Joyce, and H. Wichman, *Genetics* **187**, 185 (2011).
- [7] C. L. Burch and L. Chao, *Genetics* **151**, 921 (1999).
- [8] C. L. Burch and L. Chao, *Nature* **406**, 625 (2000).
- [9] K. Jain, J. Krug, and S.-C. Park, *Evolution* **65**, 1945 (2011).
- [10] J. E. Barrick and R. E. Lenski, *Nat. Rev. Genet.* **14**, 827 (2013).
- [11] A. Eyre-Walker and P. Keightley, *Nat. Rev. Genet.* **8**, 610 (2007).
- [12] P. D. Sniegowski and P. J. Gerrish, *Phil. Trans. R. Soc. B* **365**, 1255 (2010).
- [13] R. Korona, C. H. Nakatsu, L. J. Forney, and R. E. Lenski, *Proc. Natl. Acad. Sci. USA* **91**, 9037 (1994).
- [14] G. Fernandez, B. Clotet, and M. Martinez, *J. Virol.* **81**, 2485 (2007).
- [15] Y. Iwasa, F. Michor, and M. A. Nowak, *Genetics* **166**, 1571 (2004).
- [16] D. M. Weinreich, R. A. Watson, and L. Chao, *Evolution* **59**, 1165 (2005).
- [17] D. Rozen, M. Habets, A. Handel, and J. A. G. M. de Visser, *PLoS ONE* **3** (3), e1715 (2008).
- [18] D. R. Gifford, S. E. Schoustra, and R. Kassen, *Evolution* **65**, 3070 (2011).
- [19] D. R. Rokyta, Z. Abdo, and H. A. Wichman, *J. Mol. Evol.* **69**, 229 (2009).
- [20] J. H. Gillespie, *Theor. Popul. Biol.* **23**, 202 (1983).
- [21] J. H. Gillespie, *The Causes of Molecular Evolution* (Oxford University Press, Oxford, 1991).
- [22] D. Sornette, *Critical Phenomena in Natural Sciences* (Springer, Berlin, 2000).
- [23] J. J. Bull, and S. P. Otto, *Nat. Genet.* **37**, 342 (2005).
- [24] D. Rokyta, C. J. Beisel, and P. Joyce, *J. Theor. Biol.* **243**, 114 (2006).
- [25] R. Kassen and T. Bataillon. *Nat. Genet.* **38**, 484 (2006).
- [26] R. Sanjuán, A. Moya, and S.F. Elena. *Proc. Natl. Acad. Sci. USA* **101**, 8396 (2004).
- [27] R. C. Maclean, G. G. Perron, and A. Gardener, *Genetics* **186**, 1345 (2010).
- [28] T. Bataillon, T. Zhang, and R. Kassen. *Genetics*, **189**, 939 (2011).
- [29] M.F. Schenk, I.G. Szendro, J. Krug, and J.A.G.M. de Visser. *PLoS Genet.* **8**, e1002783 (2012).
- [30] S. Seetharaman and K. Jain, *Evolution* **68-4**, 965 (2014).
- [31] P. Joyce, D. R. Rokyta, C. J. Beisel, and H. A. Orr, *Genetics* **180**, 1627 (2008).
- [32] J. Neidhart and J. Krug, *Phys. Rev. Lett.* **107**, 178102 (2011).
- [33] K. Jain, *EPL* **96**, 58006 (2011).
- [34] A. Sousa, S. Magalhães, and I. Gordo, *Mol. Biol. Evol.* **29**, 1417 (2012).
- [35] B. Charlesworth and D. Charlesworth, *Elements of evolutionary genetics* (Roberts and Company Publishers, 2010).
- [36] K. Jain and J. Krug, *J. Stat. Mech.* , P04008 (2005).
- [37] C. Sire, S. Majumdar, and D. S. Dean, *J. Stat. Mech.* , L07001 (2006).
- [38] I. Bena and S. Majumdar, *Phys. Rev. E* **75**, 051103 (2007).
- [39] S. Sabhapandit, I. Bena, and S. Majumdar, *J. Stat. Mech.* , P05012 (2008).
- [40] H. Touchette, *Phys. Rep.* **478**, 1 (2009).
- [41] A. S. Perelson and C. A. Macken, *Proc. Natl. Acad. Sci. USA* **92**, 9657 (1995).
- [42] H. A. Orr, *J. Theor. Biol.* **220**, 241 (2003).
- [43] J. Krug and K. Jain, *Physica A* **358**, 1 (2005).
- [44] H. Flyvbjerg and B. Lautrup, *Phys. Rev. A* **46**, 6714 (1992).
- [45] K. Jain and S. Seetharaman, *Genetics* **189**, 1029 (2011).
- [46] H. A. Orr, *Evolution* **56**, 1317 (2002).
- [47] K. Jain and S. Seetharaman, *J. Nonlin. Math. Phys.* **18**, 321 (2011).
- [48] W. Feller, *An introduction to probability theory and its applications, Vol. I* (John Wiley and sons, 2000).
- [49] D. E. Knuth, *The Art of Computer Programming, Vol. I* (Addison-Wesley Professional, 1997).
- [50] C. Bender and S. Orszag, *Advanced Mathematical Methods for Scientists and Engineers* (Springer, 1999).
- [51] M. Abramowitz and I. Stegun, *Handbook of Mathematical Functions with Formulas, Graphs, and Mathematical Tables* (Dover, 1964).
- [52] H. A. Orr, *Evolution* **60**, 1113 (2006).
- [53] J. A. de Lima Filho, F. G. B. Moreira, P. R. A. Campos, and V. M. de Oliveira, *J. Stat. Mech.* , P02014 (2012).
- [54] J. Neidhart, I. G. Szendro and J. Krug, arXiv:1402.3065 (2014).

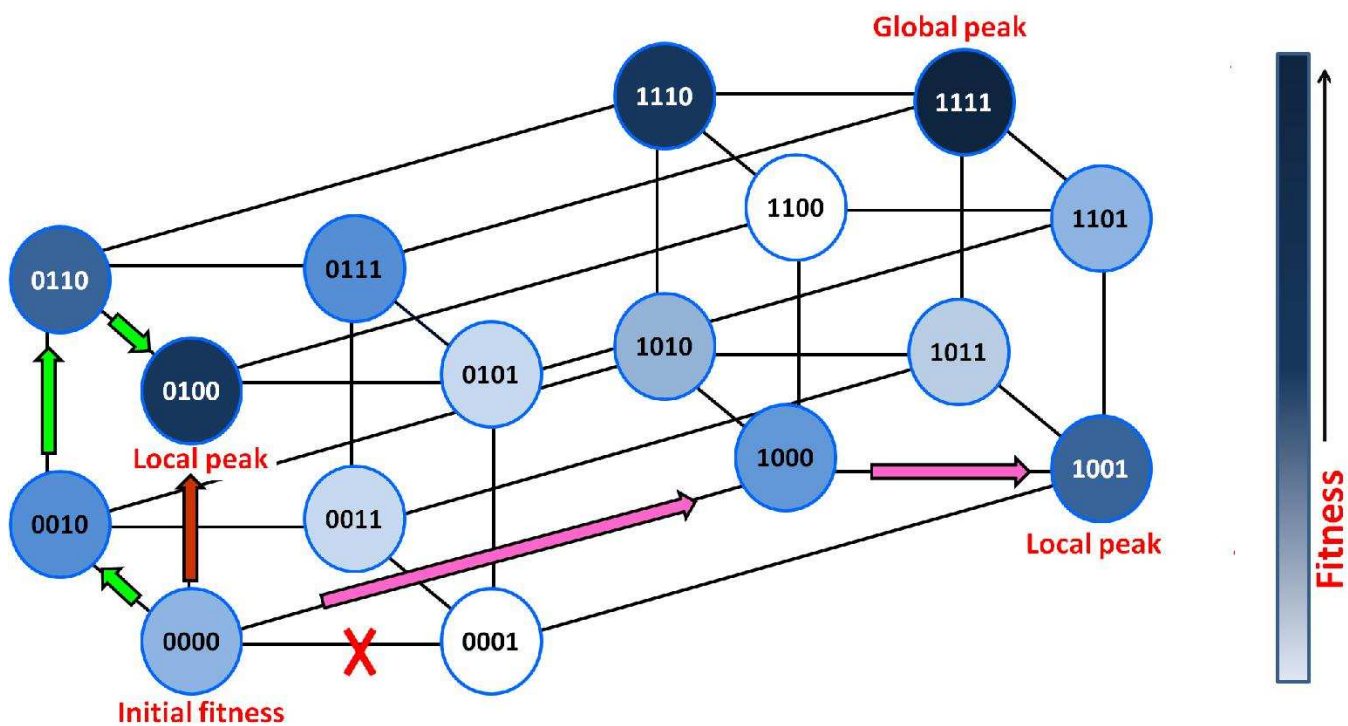


FIG. 1: (Color online) Schematic representation of adaptive walks in a 4-dimensional sequence space, starting from the same initial sequence. The arrows represent the shift of the population from a sequence to a fitter sequence one mutation away (refer text for details).

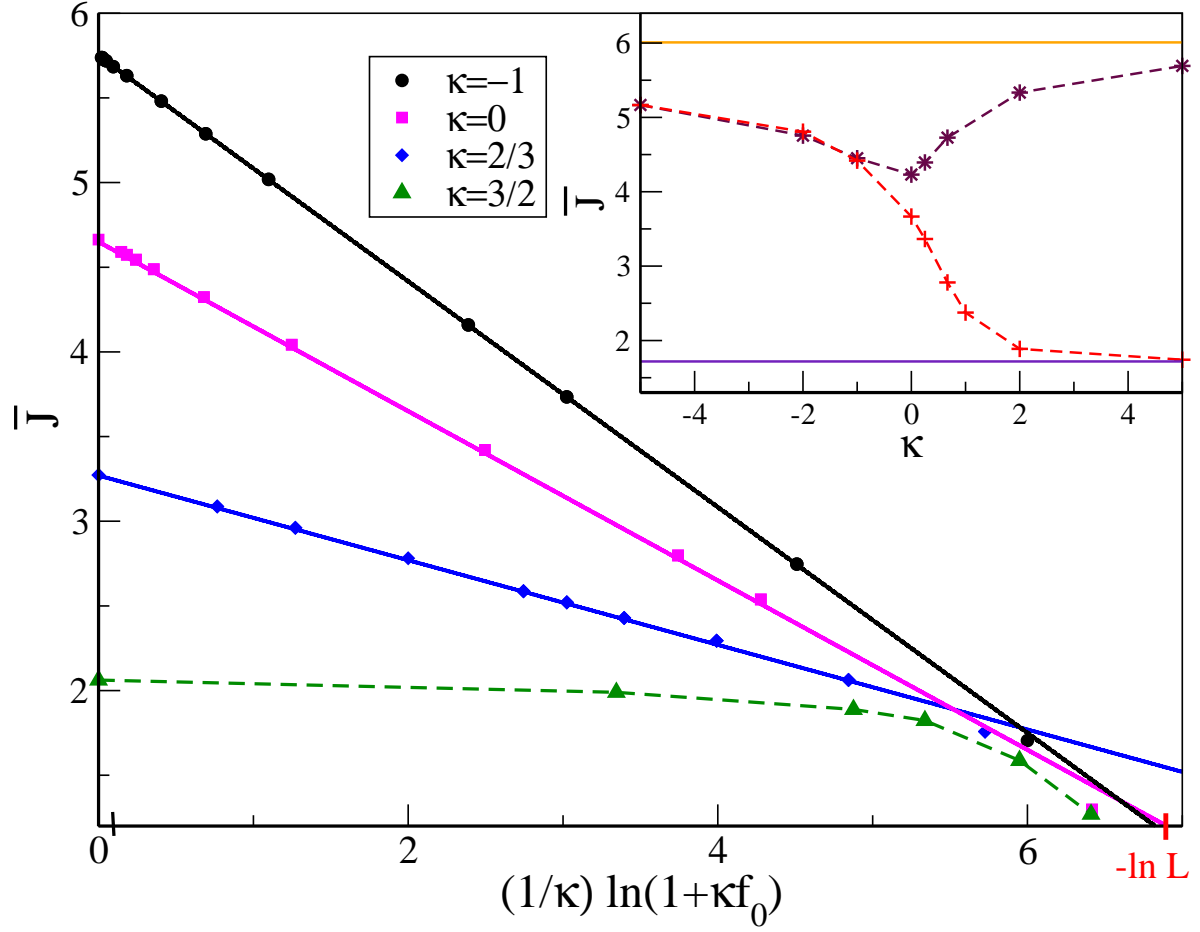


FIG. 2: (Color online) Main: Variation of the average walk length with initial fitness in the linear model on uncorrelated fitness landscapes for various κ . The simulation points are for $L = 1000$ and the lines are obtained from (31) for all $\kappa < 1$, while the one for $\kappa = 3/2$ is a guide to the eye. Inset: Comparison of the average walk length in the full model (*) and the linear model (+) for $(1/\kappa) \ln(1 + \kappa f_0) = 2$. The solid line shows the walk length expressions (8) (bottom) and (9) (top) for the greedy walk and the random adaptive walk respectively.

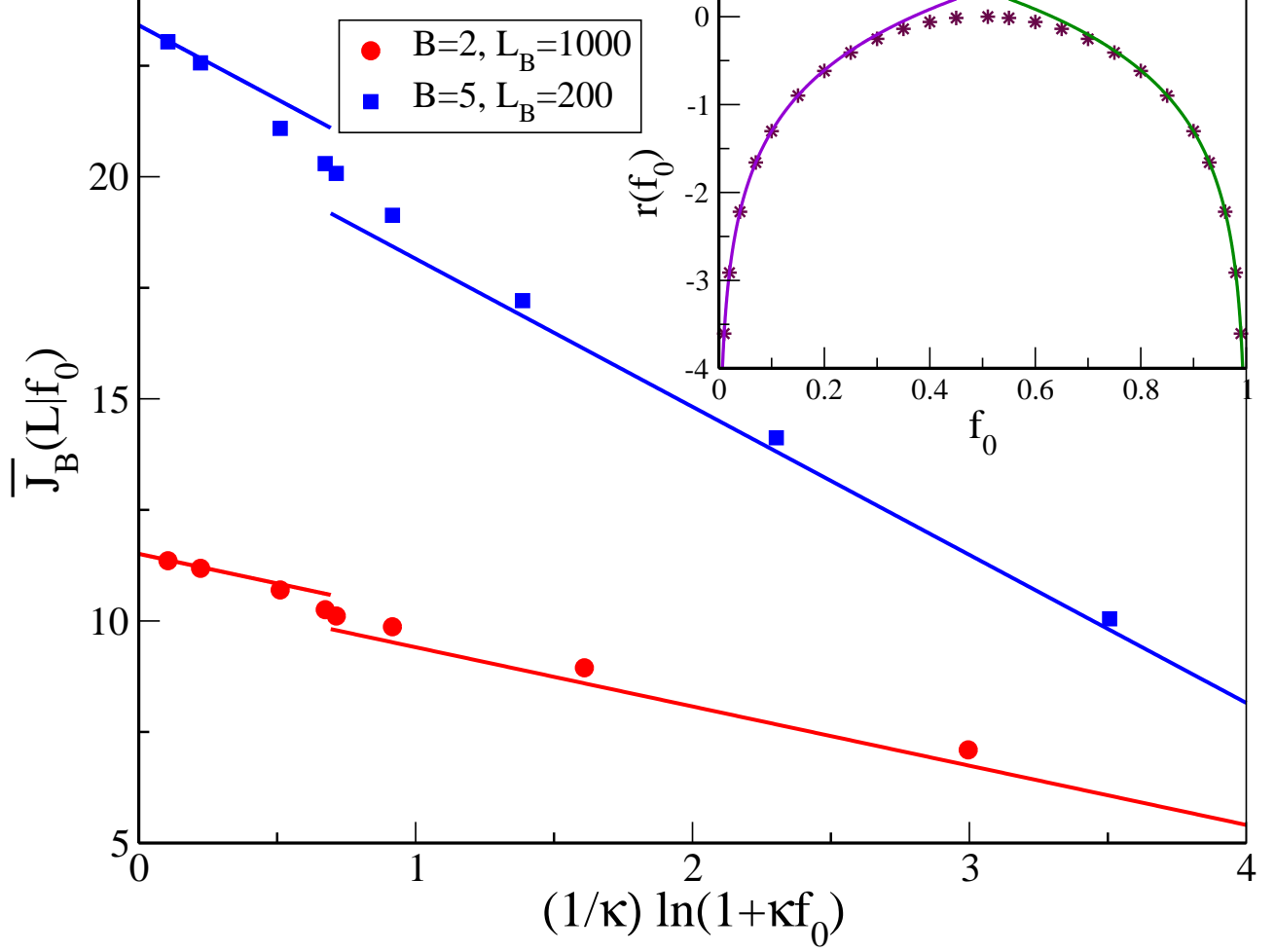


FIG. 3: (Color online) Main: Plot shows the variation of the average walk length with initial fitness for the linear model on correlated fitness landscapes for various B when $\kappa = -1$. The theoretical predictions (75) and (77) (lines) are compared against the simulation data (points). Inset: Plot shows the rate function for $\kappa = -1$ obtained using (67) and (70) (points) and the analytical formulae (72) and (73).

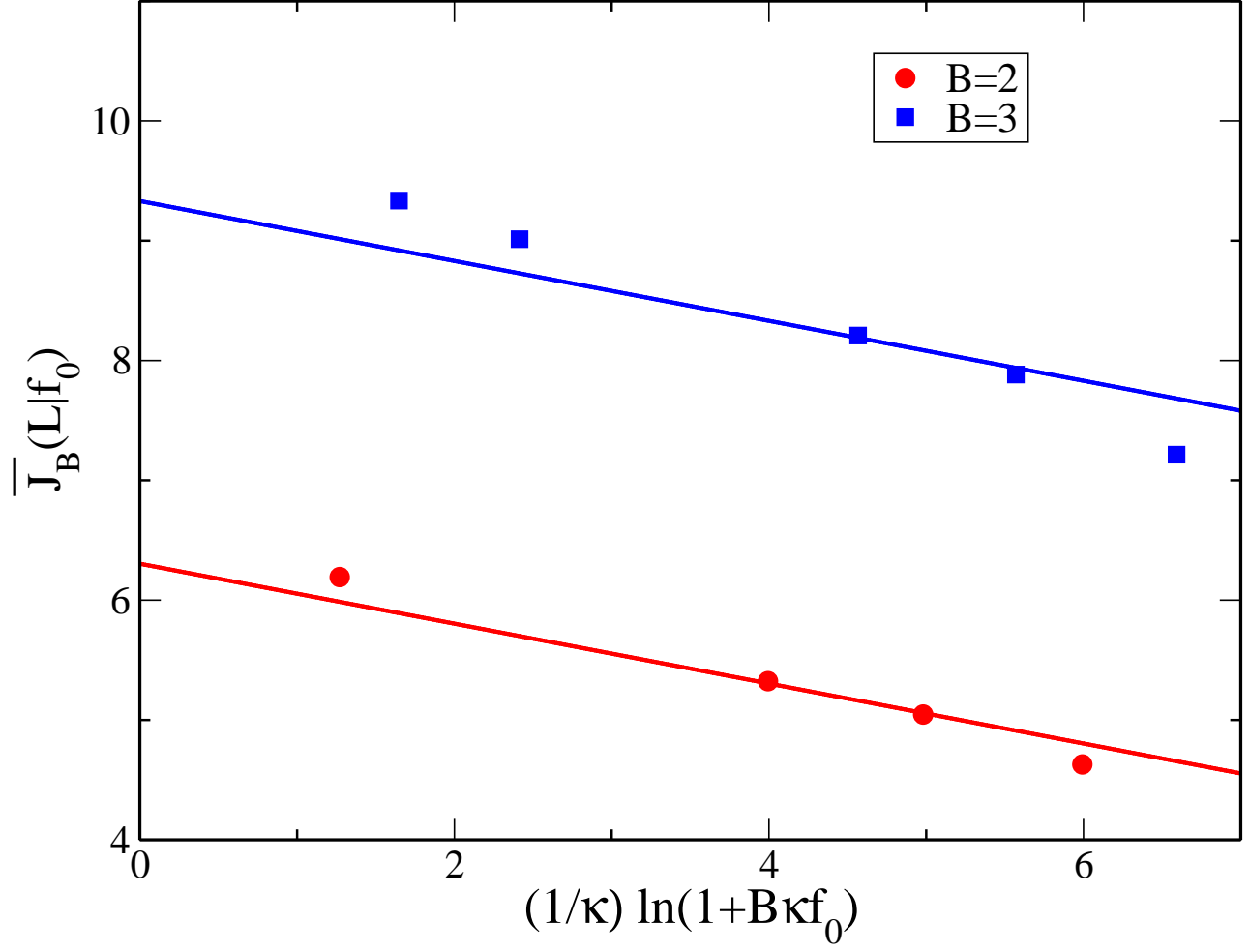


FIG. 4: (Color online) Plot shows the variation of the average walk length with the initial fitness for the linear model on correlated fitness landscapes for various B when $\kappa = 2/3$ and $L_B = 1000$. The theoretical prediction (80) (lines) is compared against the simulation data (points).

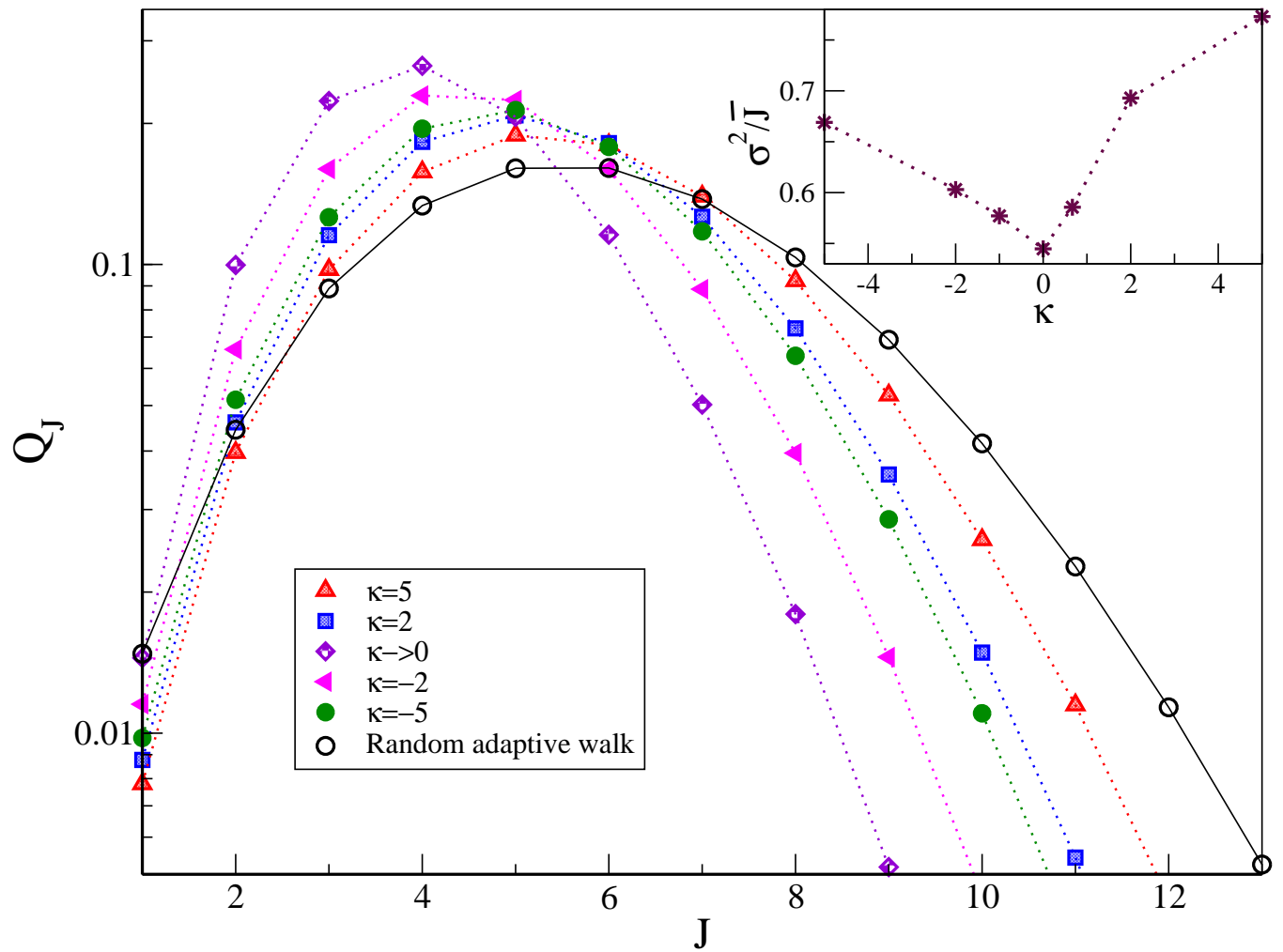


FIG. 5: (Color online) Plot to show the simulation data for the walk length distribution (main) and the index of dispersion (inset) of the walk length for various κ when $L = 1000$ using the full model on uncorrelated fitness landscapes. In the inset, $(1/\kappa) \ln(1 + \kappa f_0) = 2$.